

The Effect of Speaker Cabinet Base Support on Cabinet Vibrations

Thurman Gillespy

*Department of Physics, Edmonds Community College, Lynnwood WA 98036**

(Dated: 6 June 2016)

Speaker cabinet vibrations and resonances are known to adversely affect audio sound quality. I analyzed how six different ways of placing an audio speaker on a surface can affect the vibration of the cabinet side panel as measured with a 3-axis digital accelerometer. The strongest vibration occurred in the y-axis, in the same plane as the woofer motion. Y-axis vibrations significantly decreased when the cabinet base was more tightly coupled with the mounting surface, and x and z-axis vibrations increased. There were obvious 100 and 200 Hz resonances in the y and z-axis data in the tightly coupled mountings that were either greatly diminished or absent when the speaker base was loosely coupled. The data indicates that carefully specifying how a speaker cabinet is placed on its mounting surface is important when trying to analyze and mitigate cabinet vibrations.

PACS numbers: 43.20.Ks,43.40.Dx

Keywords: PHYS223S16;sound;resonance;accelerometer;Arduino

I. INTRODUCTION

Audio speakers generate acoustic output from one or more speaker drivers. This process can be described in terms of energy transfer (Fig 1). The amplified audio signal flows from the power amplifier to the speaker. The electrical energy (EE) of the audio signal is converted to acoustic energy (AE) by the mechanical motion (mechanical energy) (ME) of the voice coil and cone of the speaker driver. The drivers are housed in an enclosure, typically called a speaker cabinet. The cabinet provides a secure mounting for the drivers and helps contain the rearward motion of the speaker driver compresses the air inside the cabinet. Some of the stored energy in the compressed air is immediately transferred back to the speaker cone, but some is also transferred to the walls of the enclosure and is converted back into mechanical energy (in the form of vibration). In addition, the mechanical motion of the drivers (usually the woofer) directly transfers mechanical energy into the enclosure walls. The mechanical energy in the cabinet walls results in vibration and resonances [1]. The ME of the enclosure is also transferred to the surface below the cabinet.

Some of the enclosure wall mechanical energy is converted to heat through damping. The remainder is either transferred to an adjacent structure, or is converted to acoustic energy (sound) into the surrounding listening environment. This secondary acoustic output of the cabinet is added to the primary output from the drivers, and adversely affects speaker audio quality (Fig 2). Reducing cabinet vibration and resonance is an important aspect of quality audio speaker construction [2] [3]. A well designed speaker cabinet will produce a dull 'thunk' when tapped on the side.

This project is part of an ongoing effort to analyze speaker cabinet vibration, to quantitatively determine

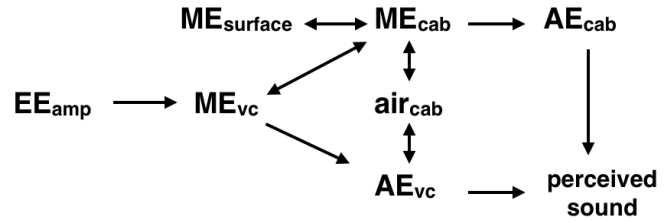


FIG. 1. Diagram of the transfer of electrical energy (EE), mechanical energy (ME) and acoustic energy (AE) in a stereo speaker. amp = audio amplifier; vc = voice coil; cab = cabinet; air = air within cabinet; surface = surface below speaker.

which methods of cabinet vibration reduction are effective, and to develop a low cost micro-controller based system that can be used by amateur audio enthusiasts. In this study, I assessed how the cabinet vibrations are affected by how the speaker is placed on a surface (upper left in Fig 1).

II. EXPERIMENT

A. Materials and Apparatus

1. Materials

1. Speaker. Model ELT525M, a 2-way speaker with 5.25" woofers and 1" tweeters from AV123.com. Speaker dimensions are 6.12" W x 11.25" H x 9.81" D. Internal loose damping material was removed from the speaker as part of a previous study (Fig 3).
2. Amplifier. CARVER AV-405 5 channel power amplifier (100 watts each channel into 8 ohms from 20Hz to 20kHz with no more than 0.08% THD).
3. Accelerometer. Freescale MMA8452Q. 3 axis, digi-

* thurman.gillespy@comcast.net

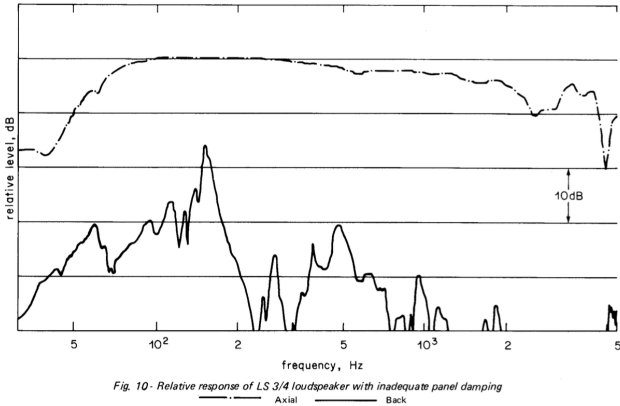


FIG. 2. Upper curve: acoustic output from speaker front. Lower curve: acoustic output from speaker rear. Acoustic output from the sides of the speaker would have been significantly larger. (Fig. 10 from Factors in the Design of Loudspeaker Cabinets, HD Harwood, R Mathews. BBC RD 1977/3.)



FIG. 3. ELT525M 2-way speaker. The woofer and tweeter have been removed from the cabinet.

tal accelerometer [4] with selectable $\pm 2g$, $4g$ and $6g$ sensitivity ranges and output data rates from 1.56 Hz to 800 Hz [5]. The device interfaces with an I²C data bus. In this experiment, the $\pm 2g$ and 800 Hz parameters were selected. The accelerometer was purchased already soldered to a small 'breakout' board [5] (Fig 4).

4. Micro-controller. Arduino UNO. A popular, low cost micro-controller that easily integrates with sensors, including digital accelerometers. The UNO

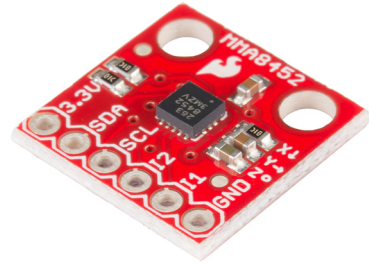


FIG. 4. MMA8452Q accelerometer mounted on a small 'breakout' board.

has an 8-bit ATmega328P processor operating at 16 MHz, with 32k flash memory and 2k of SRAM [6].

5. Shelf liner (EasyLiner, model #480617).
6. Bubble wrap. Bubble Cushioning Roll, Blue Hawk, #0167746.
7. Speaker spikes. Dayton Audio DSS2-G Gold Speaker Spike Set.
8. Cement paver. 12" x 12", Lowes Hardware.
9. Four Bench CookieTM work grippers. 1" thick x 3" diameter padded discs commonly used in wood-working. I used these to support the speaker in previous studies.

2. Apparatus

1. Hardware. A 12 inch, 4 wire ribbon cable was soldered to the accelerometer board to interface with the micro-controller. The breakout board was mounted on a small, thin piece of wood. The accelerometer and piece of wood were attached to the speaker cabinet with two wood screws (Fig 5). The accelerometer was attached to the middle of the left side panel (when viewed from the front), 3.5" from the speaker bottom. The accelerometer was oriented on the speaker such that the x-axis pointed down, the y-axis pointed toward the speaker front, and the z-axis was in the plane of the side speaker panel (Fig. 6).

The Arduino UNO was connected to the MMA8452Q accelerometer through the I²C bus. The audio output from the Arduino connected to the power amplifier through a potentiometer and audio cable (Fig 7).

2. Software. The control program was written in C/C++ using the Arduino integrated development

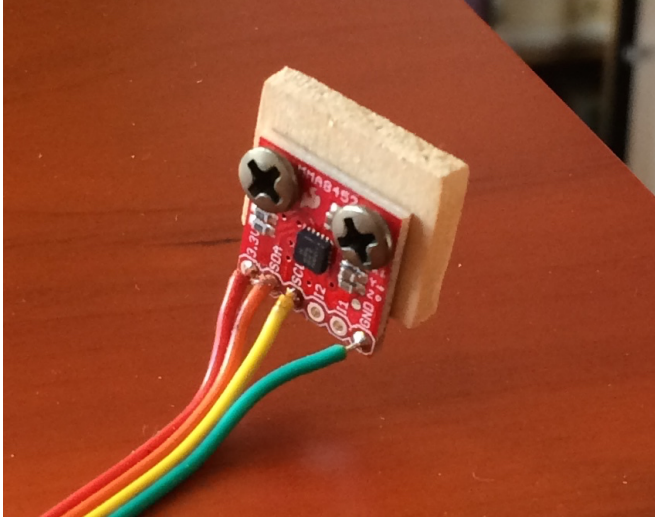


FIG. 5. MMA8452 cable and mounting assembly.

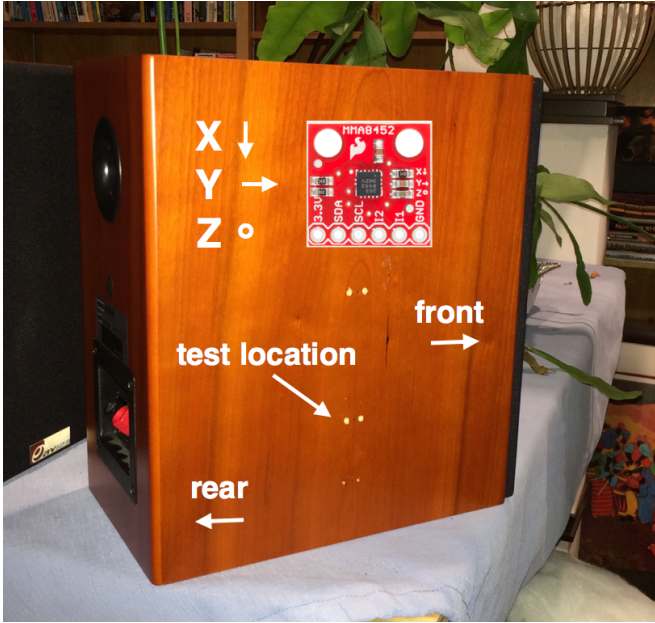


FIG. 6. Accelerometer orientation and position on the left side of the speaker. The speaker front is to the right.

environment (IDE). A 50 ms 100 Hz audio pulse was generated by the micro-controller and sent to the audio amplifier. These values were selected empirically to produce an adequate signal on the accelerometer. Immediately after the pulse began, data from the accelerometer was collected every 1.25 ms for a total of 60 samples (75 ms). The collection interval of 1.25 ms was set to match the 800 Hz output data rate of the MMA8452Q.

$$T = \frac{1}{frequency} \quad (1)$$

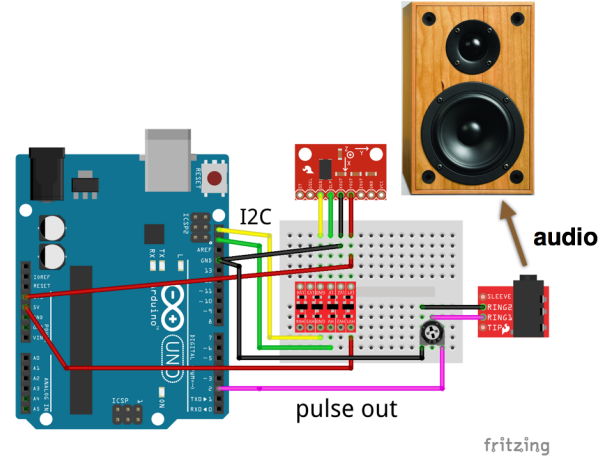


FIG. 7. System diagram. The Arduino interfaced with the system peripherals through a small breadboard.

$$\frac{1}{800Hz} = 0.00125s = 1.25ms \quad (2)$$

Before each audio pulse, 100 accelerometer data readings were collected for the x, y and z-axis, and averaged to provide a 'zero-offset' for each axis. Thus, each accelerometer reading measures the change in acceleration, Δg , from rest. The corrected accelerometer data was stored in a 3 x 60 array of 2-byte integers (*data array*).

After each pulse, rms values were calculated on the first 40 samples (50 ms) from the data array, using a standard equation for discrete values.

$$rms = \sqrt{\frac{x_0^2 + x_1^2 + x_2^2 + \dots}{n}} \quad (3)$$

These values were stored in a 3 x 15 array of 4-byte floating point numbers (*pulse array*). The data from each pulse was placed in a separate row of the array.

In addition, an rms vs time curve was calculated. For each point in the *data array*, a 3 point moving average of the rms values was calculated, and placed in a 3 x 60 array of 4-byte floating point numbers (*sequence array*). After each pulse, the new values were sequentially added to the previous values in the array.

After the 15 audio pulses, additional calculations were performed. The data in the *sequence array* was divided by 15 to calculate an average of the rms vs time data. Mean and standard deviations were calculated for the *pulse array* values.

At the end of each data collection session, the rms vs time data, and mean and standard deviation

values were transmitted over a usb serial port to a Macintosh iMac computer. The data was copied into a LibreOffice spreadsheet for data analysis and graph generation.

B. Procedure

Six different techniques for placing the speaker on a surface were tested. For each technique, 15 audio pulses were performed as described above.

1. Cement paver. The speaker was placed on the cement paver without any padding or protection of the speaker bottom. The paver weighed more than the speaker.
2. Speaker spikes (Fig 8). The speaker was placed on the paver after four speaker spikes were inserted into the speaker bottom. The spikes, cone shaped, were placed directly on the paver. The spikes were removed for all the other techniques.



FIG. 8. Speaker spike. Four spikes were installed in the cabinet base. The flat disc at the bottom of the spike was not used in this study.

3. Paver + shelf liner. A single layer of shelf liner was placed underneath the speaker.
4. Paver + bubble wrap. Two layers of bubble wrap were placed underneath the speaker.
5. Paver + work grippers. Four padded Bench Cookie™ work grippers were placed underneath the speaker. The grippers were placed under the four corners of the speaker cabinet.
6. Carpet. The speaker was placed directly on the carpet where the other measurements were obtained.

III. DATA AND ANALYSIS

Mean and standard deviations of the 50 ms pulse rms data (from the *pulse array*) are summarized in Table I and Fig 9. As expected, the y-axis, in the plane of the woofer motion, had the strongest signal.

TABLE I. 50 ms pulse, g (m/s^2) (mean \pm sd)

Method	X-axis	Y-axis	Z-axis
paver	0.128 \pm 0.001	0.222 \pm 0.036	0.095 \pm 0.012
spikes	0.130 \pm 0.010	0.223 \pm 0.027	0.119 \pm 0.001
liner	0.085 \pm 0.006	0.218 \pm 0.034	0.094 \pm 0.007
bubble	0.068 \pm 0.005	0.321 \pm 0.009	0.091 \pm 0.009
cookies	0.067 \pm 0.006	0.318 \pm 0.010	0.091 \pm 0.007
carpet	0.079 \pm 0.006	0.339 \pm 0.012	0.087 \pm 0.006

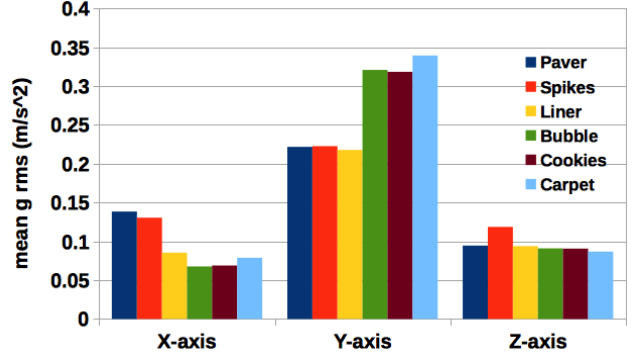


FIG. 9. Mean rms values (15 pulses) for x, y and z-axis vs mounting technique.

A. Tightly coupled vs loosely coupled

Two distinct data patterns are present: 'tightly coupled' and 'loosely coupled' speaker base to mounting surface technique. Differences in the two patterns are best illustrated by comparing the 'speaker spikes' (tightly coupled) and 'carpet' (loosely coupled) data (Fig 10, Table I).

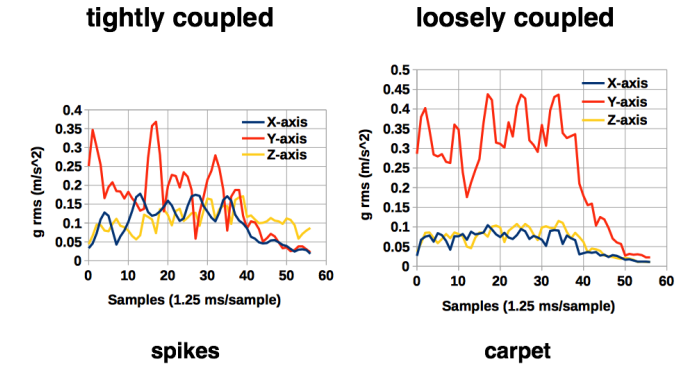


FIG. 10. Tightly coupled vs loosely coupled. The speaker spikes (left) and carpet (right) mounting methods shown to illustrate the differences between the 2 groups.

The 'tightly coupled' pattern showed significantly de-

creased y-axis vibrations compared with 'loosely coupled'. Comparing carpet with speaker spikes pulse rms data, the spikes y-axis data was 34.2% lower. Conversely, x and z-axis values increased by 64.6% and 36.8%, respectively. The pattern suggests there is increased linkage between the y-axis and the x and z-axis vibrations when the speaker base is more tightly coupled to the mounting surface. This result was completely unexpected.

The rms vs time curves of the entire measurement interval are shown in Figs 11-16.

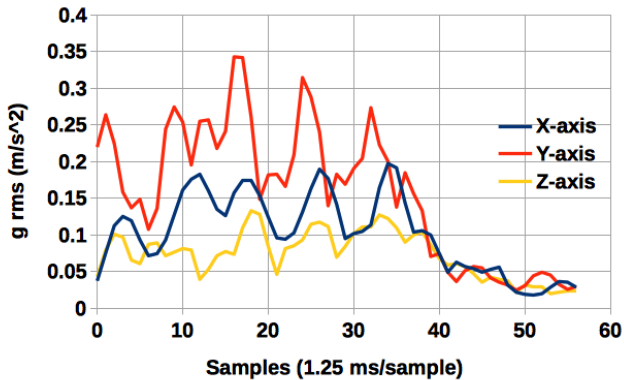


FIG. 11. Cement paver.

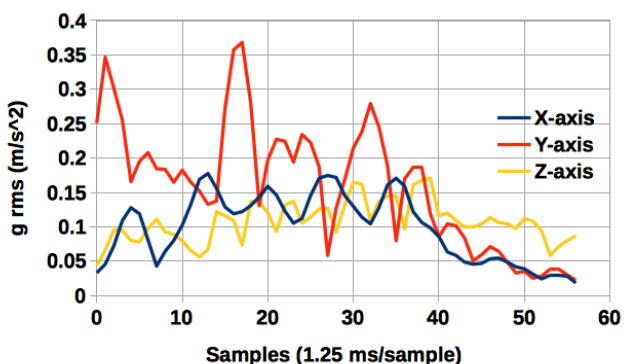


FIG. 12. Speaker spikes on cement paver.

B. Waveform analysis

The carpet y-axis rms vs time waveform had five distinct peaks, about 8 samples (10 ms) apart, which correspond to the five 100 Hz square waves during the 50 ms pulse. There is a significant dip in the rms vs time output after the second peak (centered at sample 11 or 12), consistent with a non-linear response of the woofer at that time. The x and z-axis rms vs time waveforms

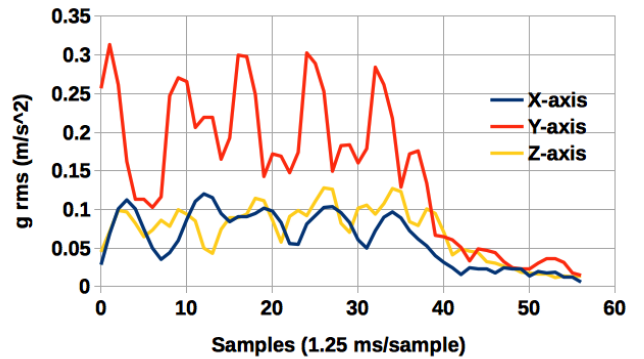


FIG. 13. Shelf liner on cement paver.

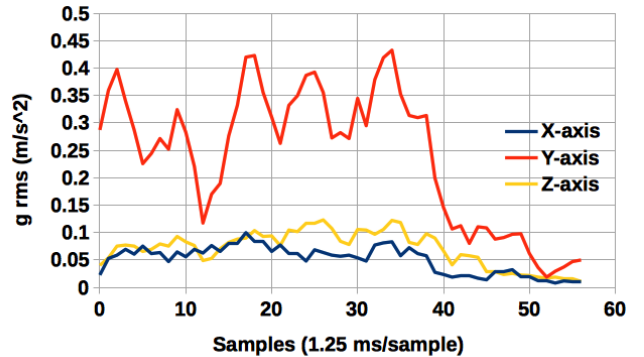


FIG. 14. Bubble wrap on cement paver.

are much smoother, indicating there is less of the 100 Hz square wave pulse influence in the signal.

In contrast, the speaker spikes y-axis waveform is more irregular, and the square wave peaks are less distinct. The x and z-axis waveforms have much stronger 'ripples' from panel resonances. In the x-axis, they occur roughly every 4 samples, which corresponds to a 200 Hz resonance. In the z-axis, they occur every 8 samples, ie, 100 Hz. However, they are delayed by 3 - 4 samples compared to the y-axis, consistent with a 180° phase shift. Paradoxically, the 'tightly coupled' mounting technique appears to induce more signal and stronger resonances in the x and z-axis compared to the 'loosely coupled' techniques.

IV. CONCLUSIONS

Analysis of speaker cabinet vibrations must take into account how the speaker is mounted on the support surface. Comparison of different techniques to reduce cabinet vibrations may need to include both a 'tightly coupled' and 'loosely coupled' mounting technique. Both conditions are commonly encountered in typical stereo systems.

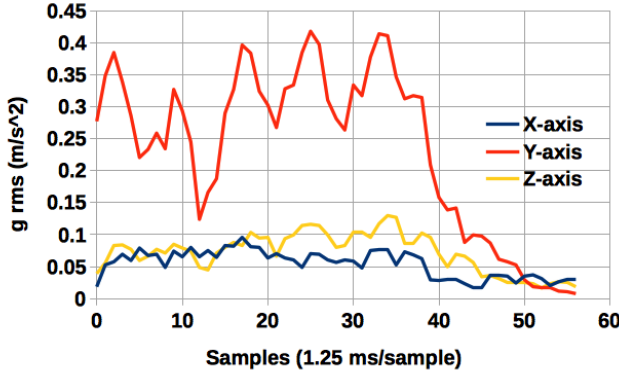


FIG. 15. Bench cookies on cement paver.

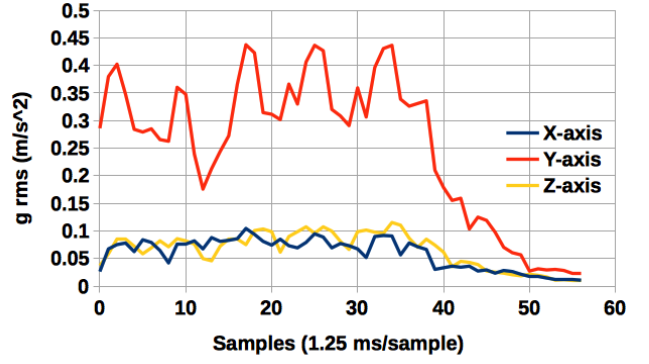


FIG. 16. Speaker on floor carpet.

V. FUTURE WORK

This project will continue with analysis of different methods of reducing speaker cabinet vibrations.

-
- [1] Resonances, *Wikipedia*. Wikimedia Foundation, 11 Feb. 2016. Web. 13 Mar. 2016.
 - [2] Colloms, Martin. *High performance loudspeakers*. Chapter 7, The enclosure. 317-328. John Wiley and Sons. 5th Ed, 1997.
 - [3] Dickason, Vance. *The Loudspeaker Design Cookbook*. Figs. 5.6 and 5.7, p102. Audio Amateur Press. 6th Ed, 2000.
 - [4] Xtrinsic MMA8452Q 3-Axis, 12-bit/8-bit Digital Accelerometer (n.d.): n. pag. Freescale Semiconductor, Inc. Web.
 - [5] SparkFun Triple Axis Accelerometer Breakout - MMA8452Q. - SEN-12756. SparkFun, n.d. Web. 13 Mar. 2016.
 - [6] Arduino UNO. Arduino - ArduinoBoardUno. ARDUINO, n.d. Web. 13 Mar. 2016.